**Supporting information**

# Defect-engineered Zr-MOFs with enhanced $O_2$ adsorption and activation for photocatalytic $H_2O_2$ synthesis

*Yong Tang, Jianhao Qiu*, Dingliang Dai, Guanglu Xia, Lu Zhang and Jianfeng Yao**

Jiangsu Co-Innovation Center of Efficient Processing and Utilization of Forest Resources, College of Chemical Engineering, Nanjing Forestry University, Nanjing 210037, China

*Corresponding author.

E-mail: jhq@njfu.edu.cn (JQ); jfyao@njfu.edu.cn (JY)

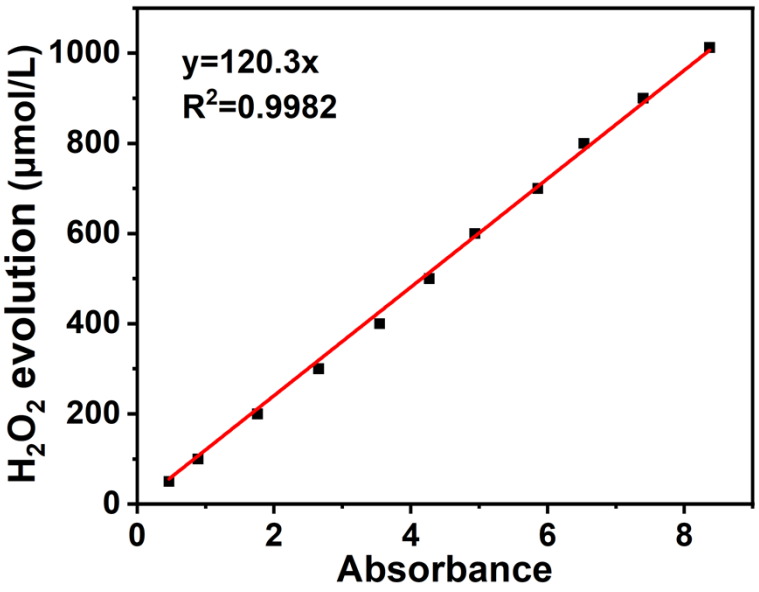


**Fig. S1** The standard curve of $H_2O_2$ concentration based on the iodometry.

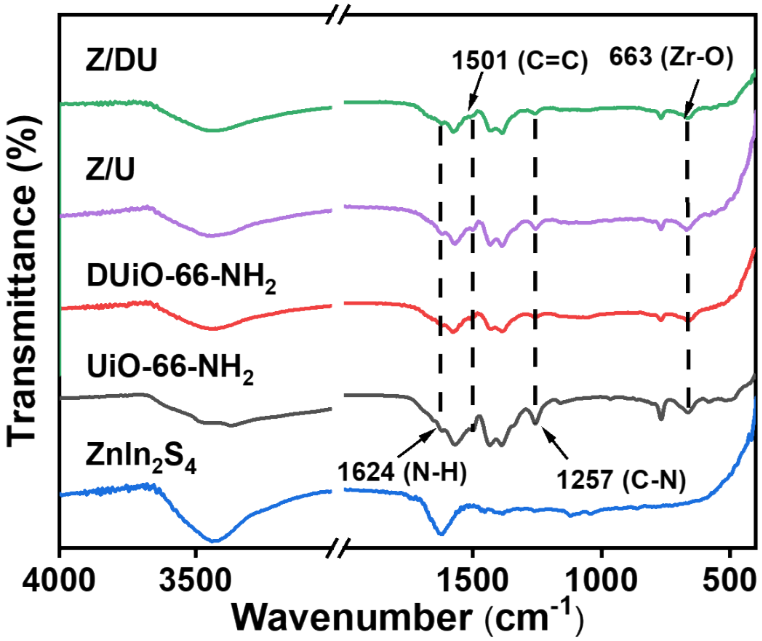


**Fig. S2** FTIR spectra of UiO-66-$NH_2$, DUiO-66-$NH_2$, $ZnIn_2S_4$, Z/U and Z/DU.

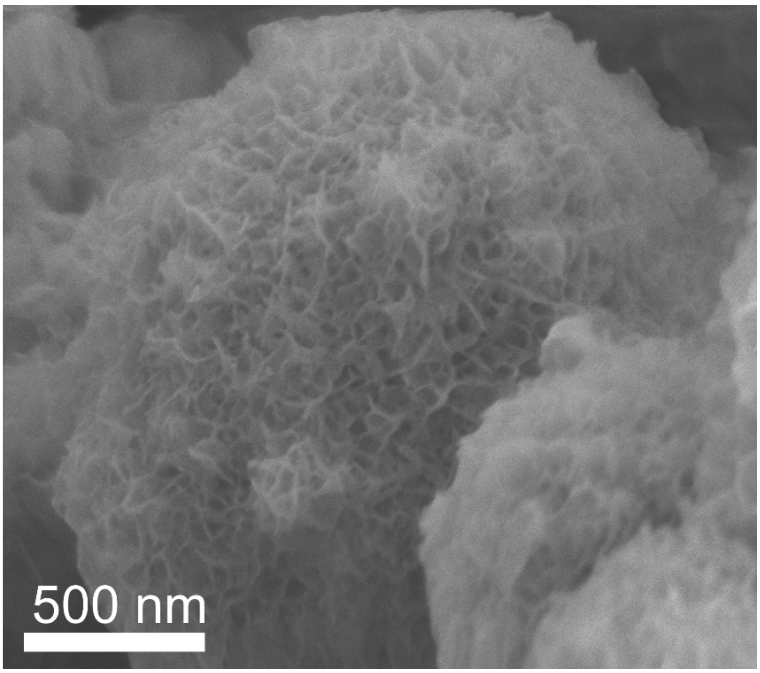


**Fig. S3** SEM image of $ZnIn_2S_4$.

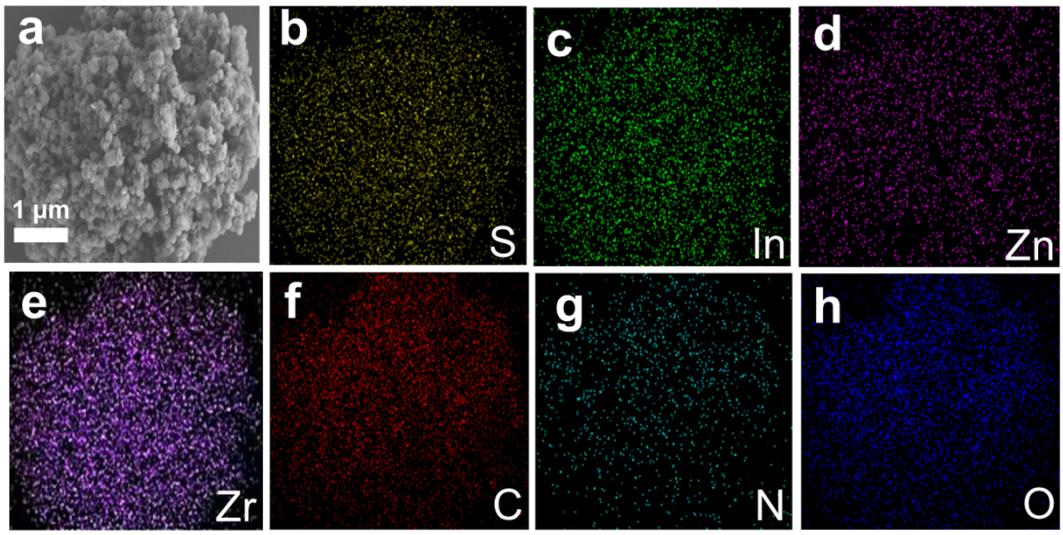


**Fig. S4** EDS mapping images of Z/UN.

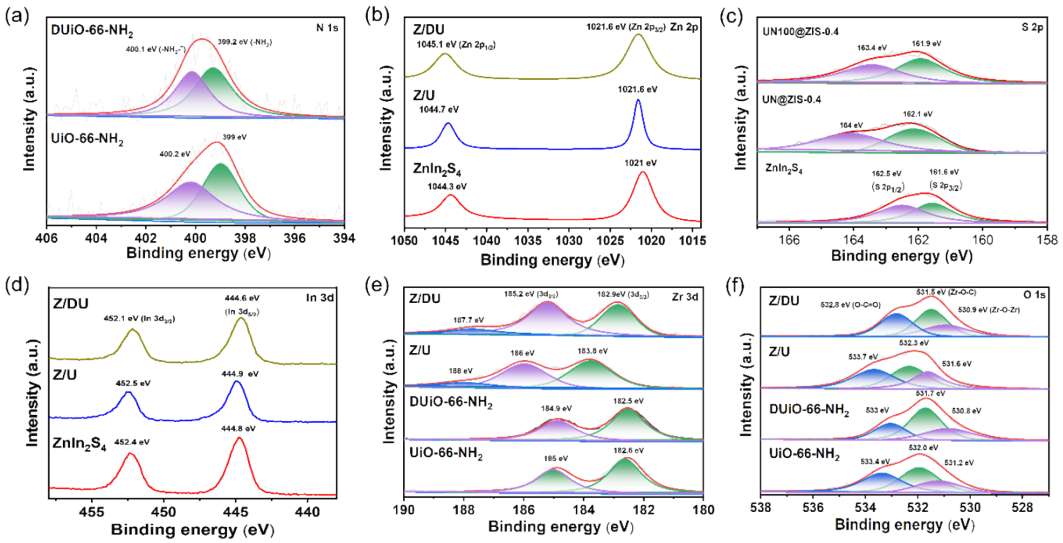


**Fig. S5** N 1s (a), Zn 2p (b), S 2p (c), In 3d (d), Zr 3d (e) and O 1s (f) XPS spectra of $ZnIn_2S_4$, UiO-66-$NH_2$, DUiO-66-$NH_2$, Z/U and Z/DU.

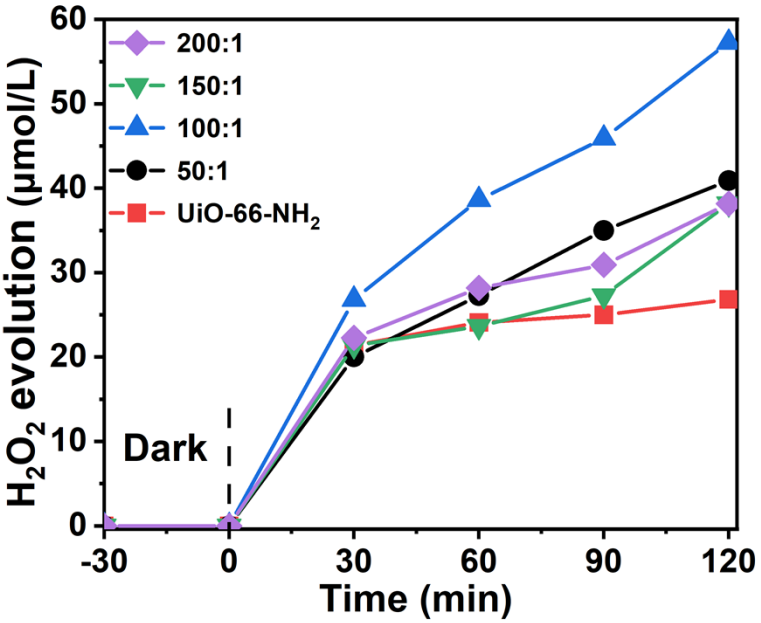


**Fig. S6** Photocatalytic $H_2O_2$ production over UiO-66-$NH_2$ and DUiO-66-$NH_2$ with HCOOH/ATA molar ratios of 50:1, 100:1, 150:1 and 200:1.

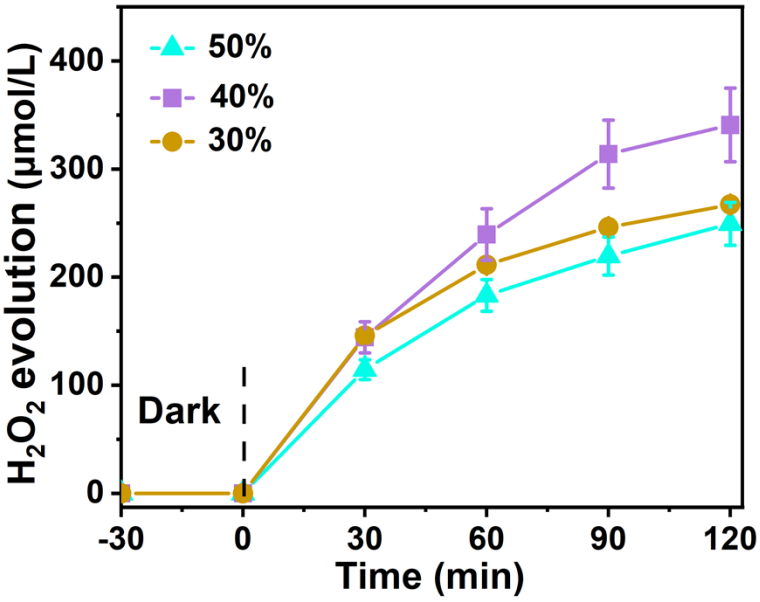


**Fig. S7** Photocatalytic $H_2O_2$ production over Z/DU with 30%, 40% and 50% weight ratio of DUiO-66-$NH_2$.

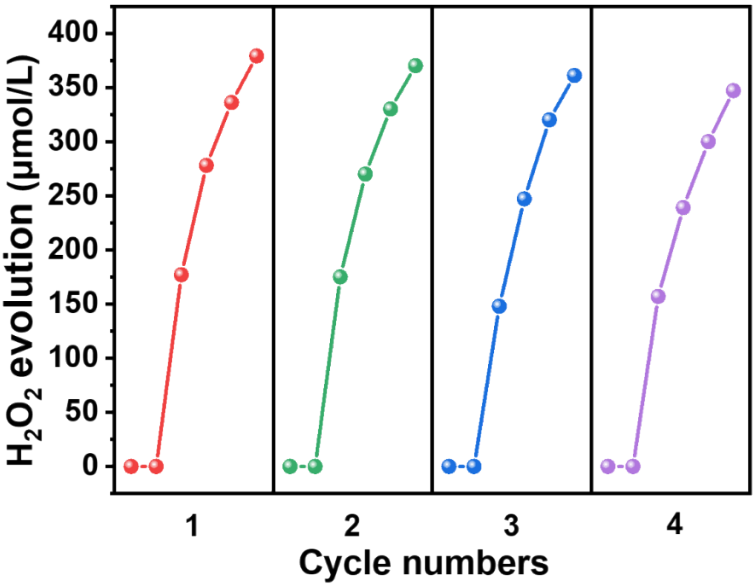


**Fig. S8** Cycle tests of Z/DU for photocatalytic $H_2O_2$ production.

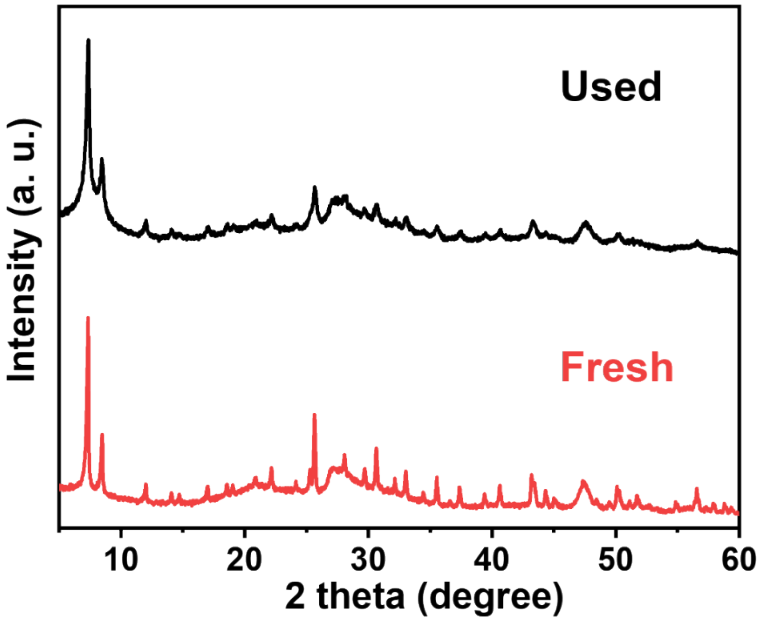


**Fig. S9** XRD patterns of Z-UN before and after cycling experiments.

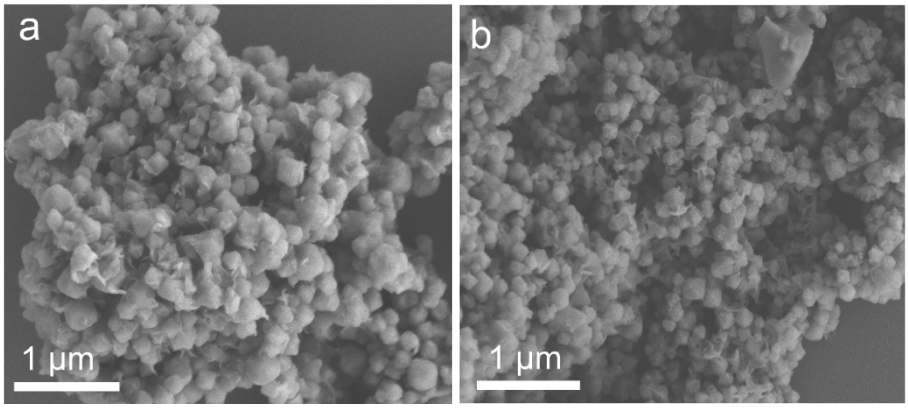


**Fig. S10** SEM images of Z/DU before (a) and after (b) photocatalytic reactions.

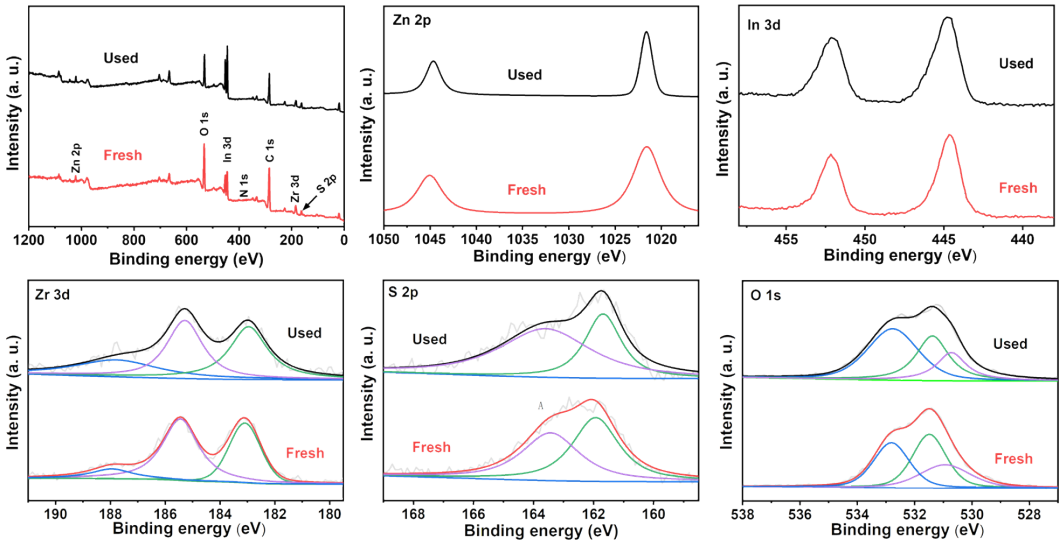


**Fig. S11** XPS spectra of Z/DU before and after photocatalytic reactions.

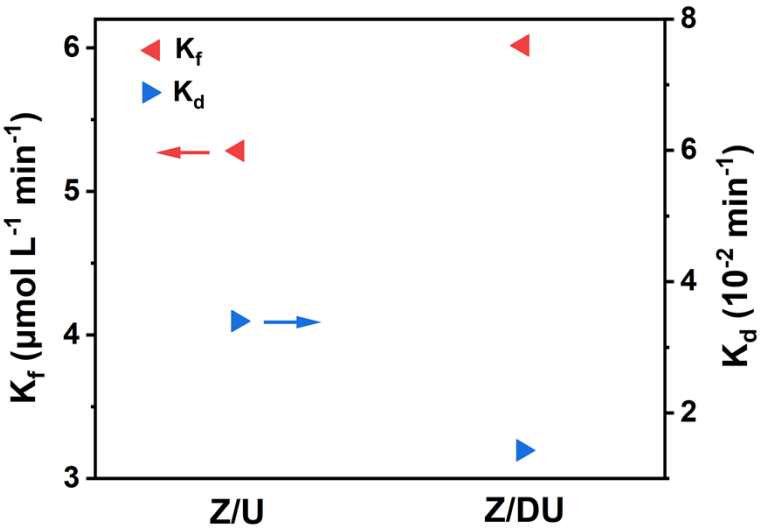


**Fig. S12** $K_f$ and $K_d$ of $H_2O_2$ over Z/DU and Z/U.

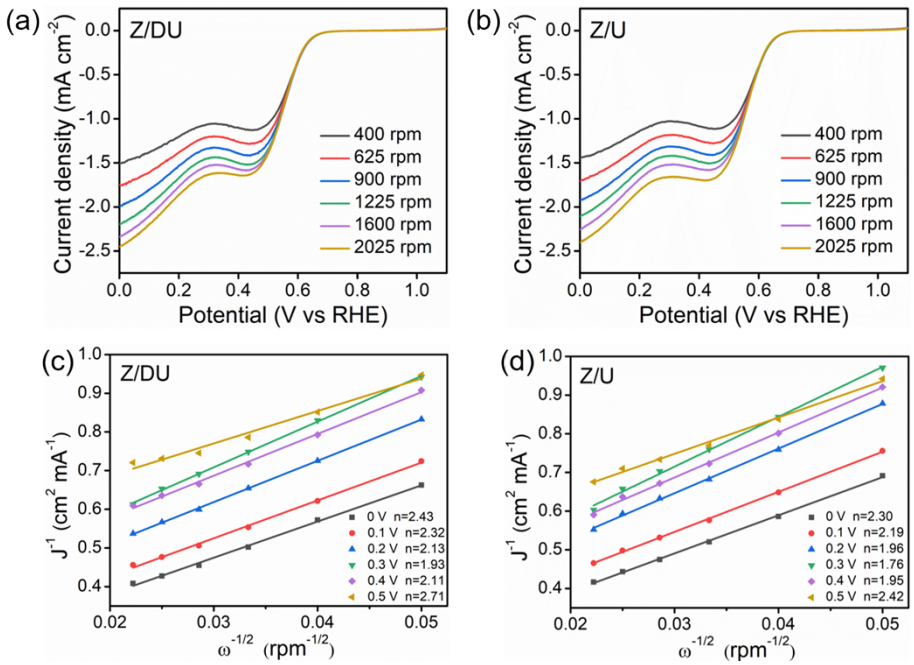


**Fig. S13** LSV curves of Z/DU (a) and Z/U (b) tested by rotating disk electrode, the corresponding fitted Koutecky-Levich plots and calculated electron transfer number of Z/DU (c) and Z/U (d) in different potentials.

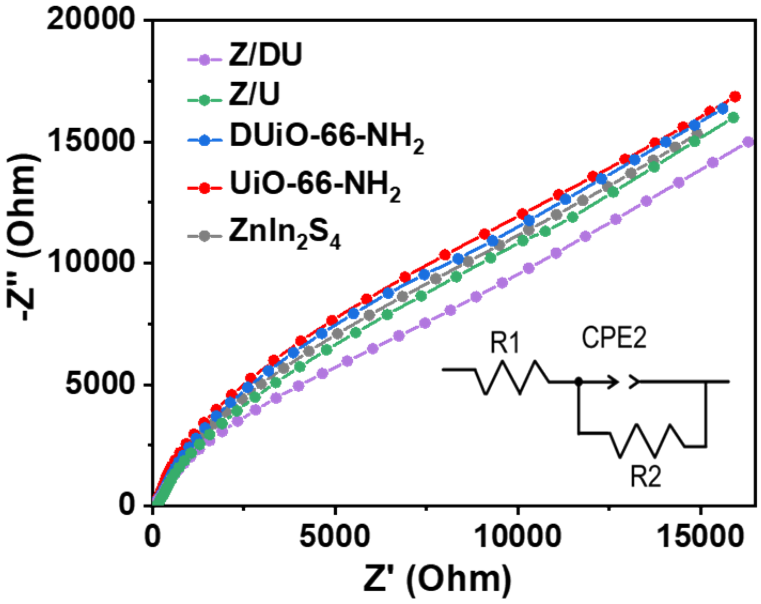


**Fig. S14** EIS Nyquist plots over $ZnIn_2S_4$, DUiO-66-$NH_2$, UiO-66-$NH_2$, Z/U and Z/DU.

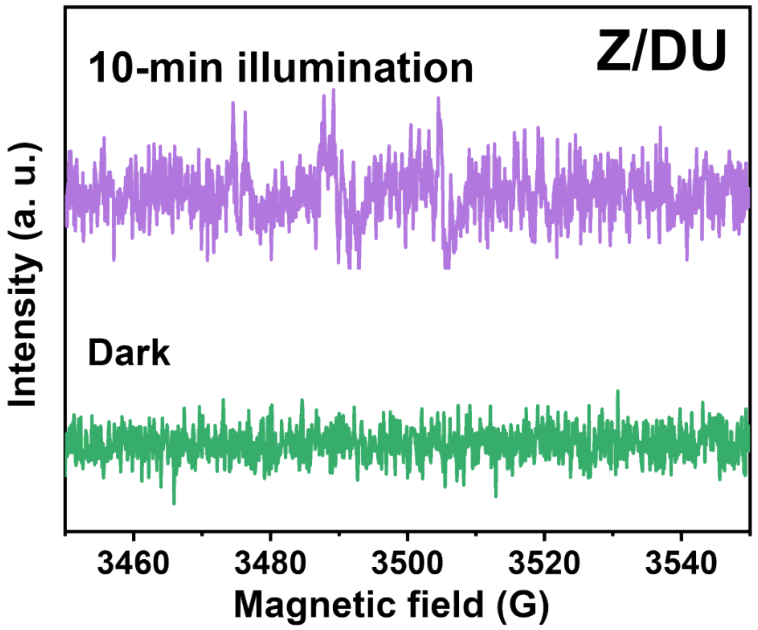


**Fig. S15** EPR spectra of DMPO-·OH adducts over Z/DU at dark and 10-min illumination.

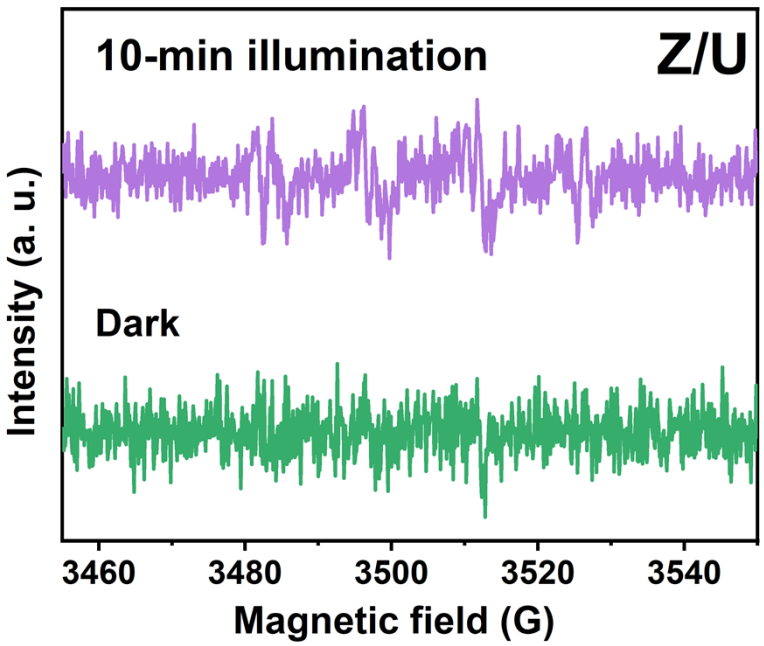


**Fig. S16** EPR spectra of DMPO-·OH adducts over Z/U at dark and 10-min illumination.

**Table S1** Data comparison of photocatalytic $H_2O_2$ production over MOF-based photocatalysts.

| Photocatalyst | Light | Sacrificial agent | Gas | Production rate ($\mu mol \cdot g^{-1} \cdot h^{-1}$) | Ref. |
|---|---|---|---|---|---|
| Ce-MIL-125-$NH_2$ | Vis | No | $O_2$ | 99 | S1 |
| Alkylated MIL-125 | Vis | Benzyl alcohol | Air | 313 | S2 |
| Ni/Hf-UiO-66-$NH_2$ | Vis | No | $O_2$ | 37 | S3 |
| MIL-125-$NH_2$($TiO_2$)/$Ti_3C_2$ | Vis | Isopropanol | $O_2$ | 278 | S4 |
| MIL-125-PDI | Vis | No | $O_2$ | 24 | S5 |
| MIL-125-$NH_2$@ZnS | Vis | Benzyl alcohol | $O_2$ | 600 | S6 |
| $C_3N_4$/MIL-101(Fe)-$NH_2$ | UV-vis | No | Air | 12 | S7 |
| MIL-88B-$NH_2$@$ZnIn_2S_4$ | Vis | No | Air | 209 | S8 |
| **Z/DU** | **Vis** | **No** | **Air** | **350** | **this work** |

## References


S1 B. Yan, S. Hu, C. Bu, Y. a. Peng, H. Han, X. Xu, Y. Liu, J. Yu and Y. Dai, *ChemNanoMat*, 2023, **9**, e20230079.

S2 Y. Isaka, Y. Kawase, Y. Kuwahara, K. Mori and H. Yamashita, *Angew. Chem. Int. Edit.*, 2019, **58**, 5402-5406.

S3 Y. Kondo, K. Honda, Y. Kuwahara, K. Mori, H. Kobayashi and H. Yamashita, *ACS Catal.*, 2022, **12**, 14825-14835.

S4 Y. Wu, X. Li, Q. Yang, D. Wang, F. Yao, J. Cao, Z. Chen, X. Huang, Y. Yang and X. Li, *Chem. Eng. J.*, 2020, **390**, 124519.

S5 X. Chen, Y. Kondo, S. Li, Y. Kuwahara, K. Mori, D. Zhang, C. Louis and H. Yamashita, *J. Mater. Chem. A*, 2021, **9**, 26371-26380.

S6 C. Liu, T. Bao, L. Yuan, C. Zhang, J. Wang, J. Wan and C. Yu, *Adv. Funct. Mater.*, 2022, **32**, 2111404.

S7 S. Su, Z. Xing, S. Zhang, M. Du, Y. Wang, Z. Li, P. Chen, Q. Zhu and W. Zhou, *Appl. Surf. Sci.*, 2021, **537**, 147890.

S8 M. Liu, Z. Xing, H. Zhao, S. Song, Y. Wang, Z. Li and W. Zhou, *J. Hazard. Mater.*, 2022, **437**, 129436.